ELSEVIER

Journal of Photochemistry and Photobiology A: Chemistry 147 (2002) 85–91

Journal of Photochemistry and Photobiology A:Chemistry

www.elsevier.com/locate/jphotochem

Mechanism of SO_2 photoionization at 193 and 308 nm in a supersonic jet

S.A. Kochubei [a], V.N. Ishchenko [b], V.I. Makarov [c,], I.V. Khmelinskii [d]

[a] *Institute of Semiconductor Physics, SB RAS, Novosibirsk 630090, Russia*
[b] *Institute of Chemical Kinetics and Combustion, SB RAS, Novosibirsk 630090, Russia*
[c] *Department of Chemistry, University of Puerto Rico, Rio Piedras Campus, P.O. Box 23346, San Juan, PR 00931-2246, USA*
[d] *Universidade do Algarve, FCT, P-8000 Faro, Portugal*

Received 11 June 2001; received in revised form 13 September 2001; accepted 1 October 2001

Abstract

In the present study, the photoionization spectrum of the SO_2 molecule in a molecular beam was studied in detail using radiation of the ArF ($\lambda = 193$ nm) and XeCl ($\lambda = 308$ nm) excimer lasers. No signals corresponding to the Van der Waals complexes or clusters of the SO_2 could be detected. The profile of the SO^+ and S^+ peaks at 193 nm could be fitted by superposition of two Gaussian functions, while at 308 nm a single Gaussian was sufficient. Power dependencies studied show that photoionization is a multiphotonic process in both cases.

Keywords: Photoionization; Excimer laser; Gaussian functions

1. Introduction

Optical excitation of Van der Waals (VdW) complexes and clusters gives an unique opportunity to study the dynamics of relaxation processes within an environment containing a limited number of particles. While it is in principle possible to control the size of the VdW clusters by adjusting the expansion conditions, it is inherently difficult to mass-select neutral clusters [1–9]. To some extent, the problem may be simplified by judiciously choosing the monomer to form the clusters. In the present paper, we studied the photoionization time of flight (TOF) mass spectra (MS) of SO_2 in pulsed molecular beams for mixtures containing 2–25% SO_2. The SO_2 molecule was photoionized by radiation of the ArF ($\lambda = 193$ nm) or XeCl ($\lambda = 308$ nm) excimer laser. The SO_2 VdW complex and cluster formation should be significant in the experimental conditions used.

UV radiation at 193 and 308 nm induces multiphoton processes in the SO_2 molecule, involving the $\tilde{C}^1B_2 \leftarrow \tilde{X}^1A_1$ and $\tilde{B}^1B_1 \leftarrow \tilde{X}^1A_1$ transitions as the first step. Okabe [10] showed that the SO_2 photodecomposition under excitation of the $\tilde{C}^1B_2 \leftarrow \tilde{X}^1A_1$ transition proceeds as a predissociation process, induced by nonadiabatic interaction between levels of the $\tilde{C}^1B_2$ and $\tilde{X}^1A_1$ states. This conclusion was obtained by analyzing the wavelength dependence of the fluorescence quantum yield. In particular, the fluorescence quantum yield was falling off very sharply beyond 219 nm. This conclusion has been confirmed by Hui and Rice [11], who found that at lower wavelengths the fluorescence quantum yield goes down accompanied by the fluorescence lifetime decrease from 40 to 8 ns as the excitation energy becomes higher than the predissociation energy. Analysis of the fluorescence excitation spectrum of SO_2 in collisionless conditions allows one to determine exactly the predissociation energy interval of SO_2, the low limit of which corresponds to 543 kJ/mol (45 400 cm^{-1}) [12]. Studying population of the spin-sublevels of the $SO(\tilde{X}^3\Sigma^-)$ radical, the predissociation process was shown [13] to involve the $^3A'$ state, i.e. crossing of the singlet and triplet surfaces of the SO_2 molecule. Abe and Hayashi [14] studied magnetic field influence on the SO_2 fluorescence under excitation of this molecule close to the predissociation limit. They showed [14] that the magnetic field effect increases with increase of the excess of the vibrational energy above the (0,0,0) $\tilde{C}^1B_2$ level, almost vanishing at excitation energies higher than the predissociation limit. The observed data have been explained using the direct mechanism theory [15,16] in the frameworks of which an external magnetic field induces coupling between levels of the excited and ground states. The magnetic field effect disappears when the rate of the magnetic field-induced processes becomes much smaller than that of the natural predissociation process. Note that under excitation of the SO_2 molecule below the predissociation limit the quantum beat effects have been observed for the distinct rovibronic

[1] Corresponding author. Tel.: +1-787-764-0000x2858/7671; fax: +1-787-756-7717.
E-mail address: makarov@adam.uprr.pr (V.I. Makarov).

1010-6030/02/$ – see front matter
PII: S1010-6030(01)00613-X

levels excited [17]. These effects have been explained using an interaction scheme, whereby levels of the excited and ground states are coupled by intramolecular interactions.

Study of the photodissociation processes of the SO_2 molecule excited by radiation of the ArF excimer laser ($\lambda = 193$ nm) was carried out by Freedman et al. [18] and Kawasaki and Sato [19]. These authors studied photodissociation process of the SO_2 molecule using the molecular beam (MB) and time of flight mass-spectrometry (TOF MS) methods, measuring velocity distribution of the photodissociation products. The SO_2 photofragmentation from the $\tilde{C}^1B_2$ state was shown to occur via predissociation from discrete levels of the $\tilde{C}^1B_2$ state to the dissociative continuum of the $\tilde{X}^1A_1$ ground state. However, possible role of intermediate singlet and triplet states has not been ruled out.

Two-photon dissociation of SO_2 excited by radiation of the KrF and XeCl excimer lasers has been studied by Effenhauser et al. [20]. In these cases, the SO and O intermediates may be produced in different states, excited states including ($SO(\tilde{X}^3\Sigma^-)$, ($\tilde{a}^1\Delta$), ($\tilde{b}^1\Sigma^+$); $O(^3P)$ and (^1D)), i.e. products of the SO_2 photodissociation may consist energy excess distributed by different degrees of freedom of SO and O. Besides, the process

$$SO_2 + 2h\nu_{KrF} \rightarrow S + O_2 \quad (1)$$

is possible under excitation of SO_2 by radiation of the KrF excimer laser ($\lambda = 248$ nm). Here, the S and O_2 species may be produced as well in different states. Note that these processes have not been studied in detail yet.

The two-photon ionization mechanism of the SO_2 is poorly known. The only work by Wang and Lee [21] studied photocurrent induced by radiation of the ArF excimer laser in the 250 Torr N_2 + 33.6 mTorr SO_2 mixtures. They determined the cross-section value of the two-photon ionization of SO_2 at 193 nm. Thus, it should be of interest to study the detailed mechanism of two-photon ionization of SO_2, as well as the dynamics of the VdW complex and cluster formation for the SO_2, using two-photon ionization to detect these particles.

Here, we studied the SO_2 photoionization using radiation of the ArF and XeCl excimer lasers, a collimated pulsed molecular beam and TOF MS detection. The TOF mass spectra were taken in different experimental conditions. The data obtained were qualitatively explained by concurrent photodissociation and photoionization of the VdW complexes and clusters as well as of the SO_2 molecule.

2. Experimental

General schematic representation of our experimental setup is shown in Fig. 1a. The laser radiation entered the work region of the vacuum chamber via stainless steel tubes covered by quartz windows mounted at 60° to the tube axis. Laser radiation was perpendicular to the molecular beam direction. Products were detected in a direction perpendicular to both the laser radiation and the molecular beams. Ions produced by laser radiation were separated and detected by a home-made time of flight mass-spectrometer (TOF MS), schematic representation of which is shown in Fig. 1b. The resolution of the TOF MS was about 350. A VEU-7 secondary electron multiplier and an MCP (20 mm inlet aperture, Hamamatsu) were used for ion detection. Multiphoton ionization was initiated by a home-made ArF laser and an LPX-200 XeCl laser (Lambda-Physics). The laser pulse duration was 5–7 and 15–20 ns, and the maximum pulse energy was 0.5 and 170 mJ, for the respective ArF and XeCl systems. A lens system was used for focusing the laser beam into the photoionization volume of the TOF MS system. The photoionization volume had a cross-section of 1.0×0.5 mm^2. Home-made electrodynamic and commercial electromagnetic (general valve series 9) pulsed valves were used to shape the gas pulse, achieving pulse duration of 250 μs. The sonic nozzle diameter was 250 μm, with 15 mm nozzle to skimmer inlet aperture distance. The skimmer aperture was about 2 mm in diameter, with the aperture to the photoionization region distance of 60 mm. Molecular beam was generated using different buffer gases (He, Ne, Ar, Kr, N_2, CH_4) containing between 2 and 25% of the SO_2. The total pressure was varied in the range 1–4 atm. Translational axial temperature was measured using an optical method described earlier [22], yielding values between 1 K (Ar + 25%SO_2; $P_0 = 1.2$ atm) and 3 K (Ne + 25%SO_2; $P_0 = 2$ atm).

Data acquisition was performed using DVK-3 PDP-compatible and pentium PC microcomputers, connected to an ADC, LeCroy oscilloscope, boxcar integrator, and other devices via a CAMAC or GPIB interface. Time resolution of the detection system was 12.5 or 2.5 ns. Measured TOF MS data were normalized to the total energy of the laser pulse. The TOF signals were recorded both with and without the sample, $I_s(t)$ and $I_b(t)$, respectively, and the TOF mass spectrum subsequently calculated as $I_s(t) - I_b(t)$. The SO_2 was obtained using the reaction of Na_2SO_3 with H_2SO_4, and purified by vacuum trap to trap distillation. Commercial SO_2 (Air Products) was used without additional purification.

3. Results

In the present study, the TOF mass spectra (MSP) of the X + 20%SO_2 mixtures were measured in different experimental conditions for X = He, Ne, Ar, Kr, N_2, CH_4 buffer gases. Laser power curves were taken for different spectral peaks.

3.1. Time of flight mass spectra

The TOF MSP were recorded under different experimental conditions. A typical spectrum obtained for the Ar + 20%SO_2 mixture at $P_0 = 1$ atm and $\lambda = 193$ nm is shown in Fig. 2a. As it can be seen, the spectrum contains only

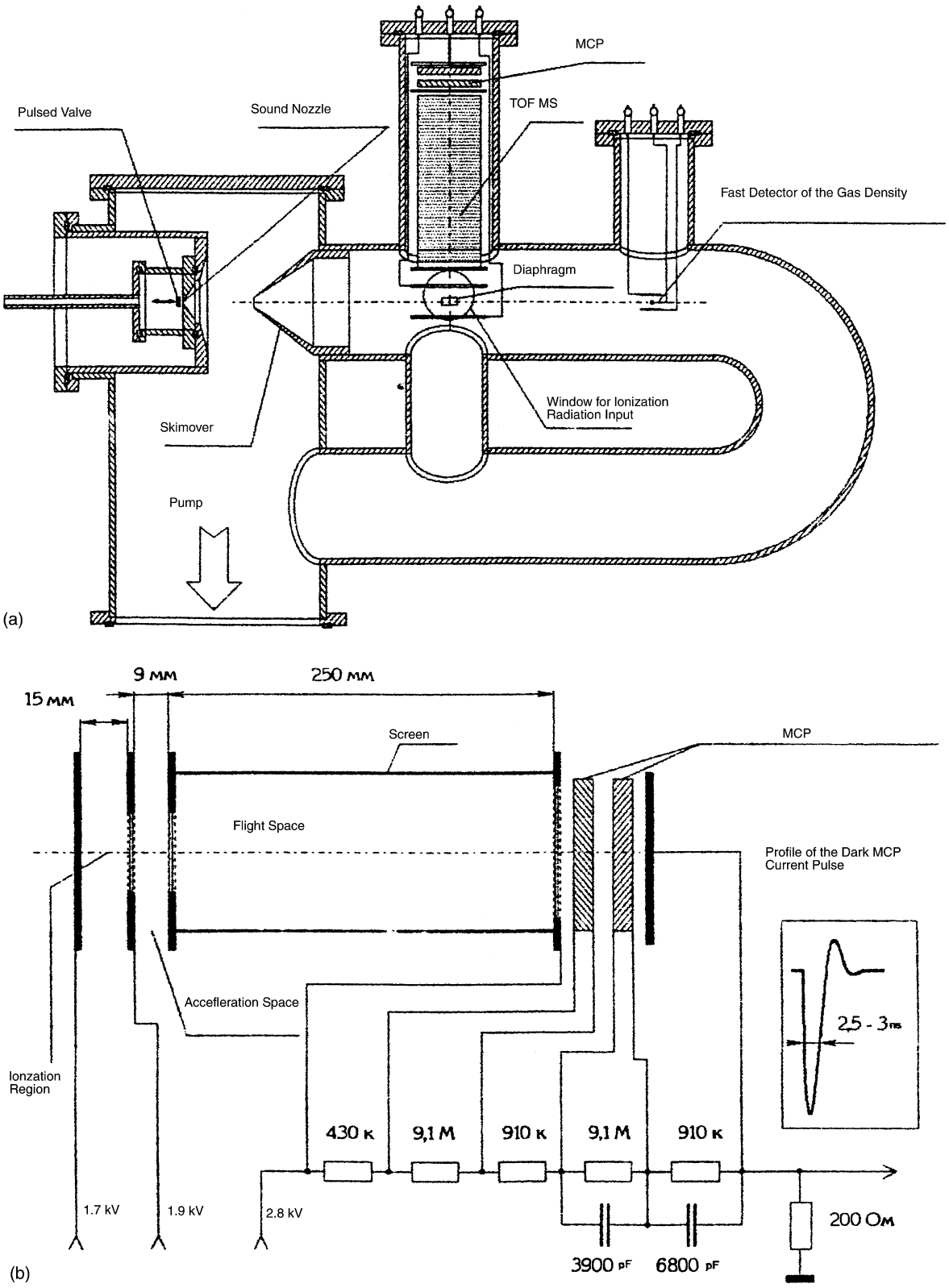

Fig. 1. Schematic representation of the experimental setup: (a) the vacuum chamber and the TOF MS; (b) the TOF MS scheme.

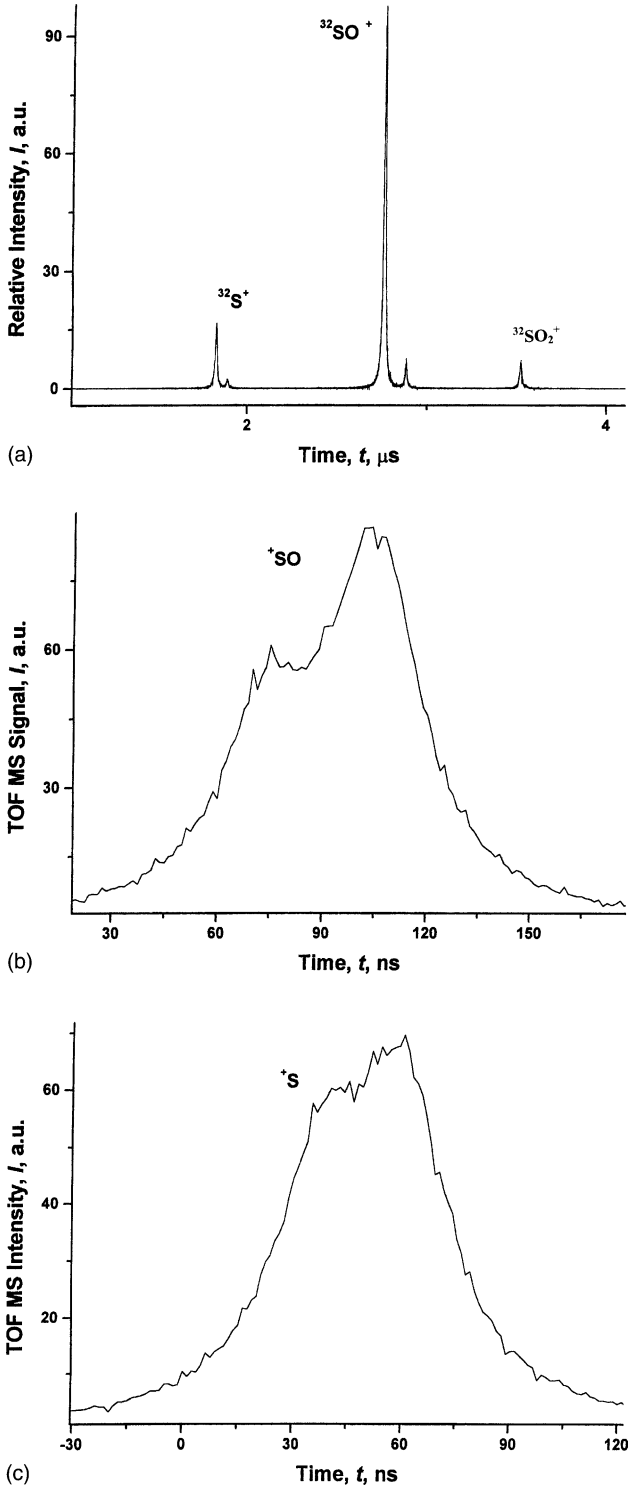

Fig. 2. The SO_2 TOF mass spectra obtained for the Ar+20%SO_2 mixture at $P_0 = 1$ atm and $\lambda = 193$ nm: (a) the complete spectrum; (b) detailed structure of the SO^+ peak; (c) S^+ peak.

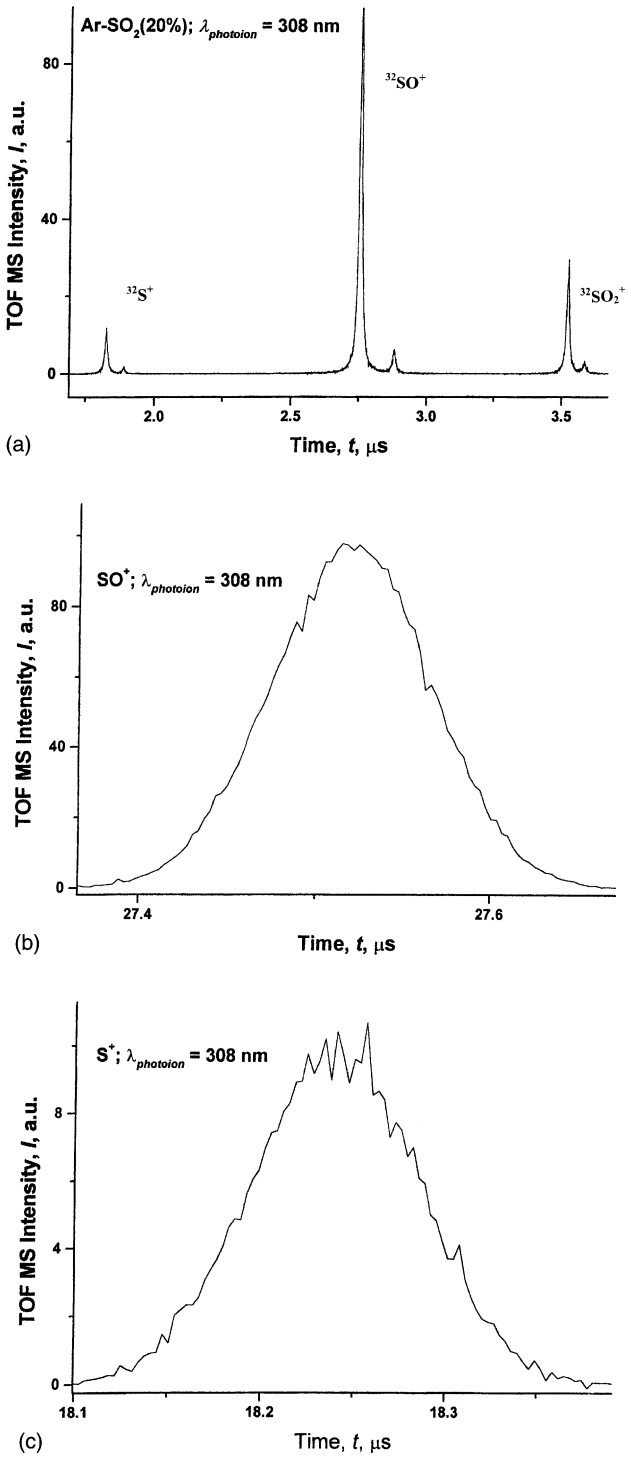

Fig. 3. The SO_2 TOF mass spectra obtained for the Ar+20%SO_2 mixture at $P_0 = 1$ atm and $\lambda = 308$ nm: (a) the complete spectrum; (b) detailed structure of the SO^+ peak; (c) S^+ peak.

three main peaks corresponding to the ^{32}S isotope—32 amu ($^{32}S^+$), 48 amu ($^{32}SO^+$) and 64 amu ($^{32}SO_2{}^+$), with 16:97:6 relative intensities. No peaks of VdW complexes or clusters were observed in the range of experimental conditions used. High-resolved TOF MSP of the 48 amu ($^{32}SO^+$) and 32 amu ($^{32}S^+$) peaks are shown in Fig. 2b and c, respectively, demonstrating a complex structure. Each of these peaks may be represented by a sum of two Gaussian components shifted by 18 and 25 ns for the respective 32 amu ($^{32}S^+$) and 48 amu ($^{32}SO^+$) peaks. We shall discuss possible nature and reasons concerning this structure later.

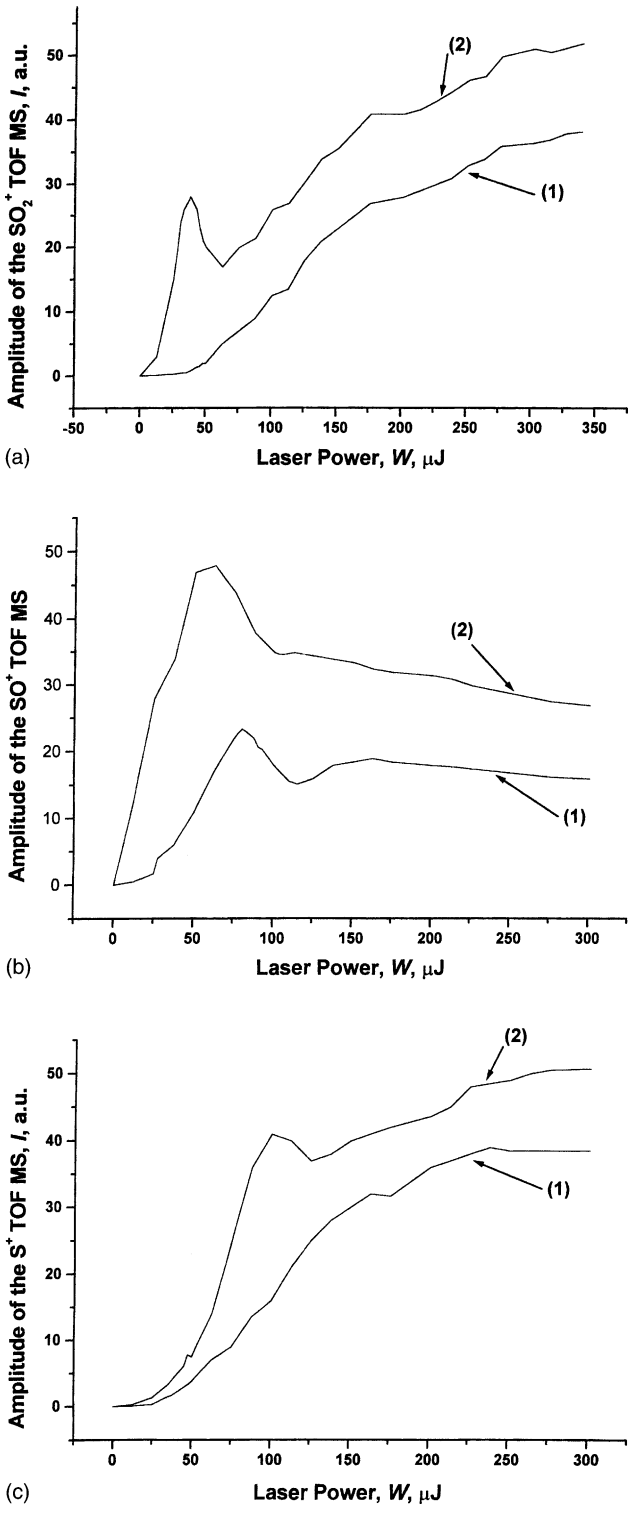

Fig. 4. Dependences of the peak intensity on the laser power measured for the Ar+20%SO_2 mixture at $\lambda = 193$ nm, $P_0 = 1$ atm: (a) 1—background, 2—64 amu peak (SO_2^+); (b) 1, 2—first and second components of the 48 amu peak (SO^+); (c) 1, 2—first and second components of the 32 amu peak (S^+).

Typical spectrum taken for the Ar + 20%SO_2 mixture at $P_0 = 1$ atm and $\lambda = 308$ nm is shown in Fig. 3a. This spectrum was shifted into the time range of Fig. 2a. The TOF spectrum contains only three main peaks corresponding to the ^{32}S isotope—32 amu ($^{32}S^+$), 48 amu ($^{32}SO^+$) and 64 amu ($^{32}SO_2{}^+$), with 10:97:26 relative intensities. Once more, no peaks attributable to VdW complexes or clusters were observed. High-resolved spectra of the 48 amu ($^{32}SO^+$) and 32 amu ($^{32}S^+$) peaks are shown in Fig. 3b and c, respectively. This time each peak may be described by a single Gaussian component. Thus the results are qualitatively different for the two ionization wavelengths employed.

3.2. Peak intensity as a function of the laser power

Dependences of the peak intensity on the laser power were measured in the present study. Typical curves obtained for the Ar + 20%SO_2 mixture at $\lambda = 193$ nm, $P_0 = 1$ atm are shown in Fig. 4. Fig. 4a shows the intensity curves for the background (1) and the 64 amu (2) signals; Fig. 4b—those for the first (1) and second (2) components of the 48 amu signal, and Fig. 4c—for the first (1) and second (2) components of the 32 amu signal. All the curves are complex functions of the laser power to be analyzed in detail later. Here, the first and second components mean the first and second (by the time scale) peaks of the 48 and 32 amu signals. Power dependences for $\lambda = 308$ nm are shown in Fig. 5a–c for the respective $SO_2{}^+$, SO^+ and S^+ signals. The respective plots present monotonous curves, making the two wavelengths qualitatively different.

4. Data analysis and discussion

This section will present a qualitative analysis of the experimental results.

4.1. The TOF mass spectra

Spectra recorded both at 193 and 308 nm only contain signals corresponding to the $SO_2{}^+$, SO^+ and S^+ ions, without any signals attributable to VdW complexes or clusters. Note also that the amplitude of the $SO_2{}^+$ signal is much smaller than that of SO^+, comprising about half of the S^+ signal at 193 nm. However, the relationship between amplitudes of the SO^+ and S^+ peaks is reversed at $\lambda = 308$ nm. To explain the absence of the VdW complexes and clusters, we assume that the photoionized VdW complexes and clusters get excited and becoming unstable, decompose quickly in a few picoseconds, producing the observable $SO_2{}^+$, SO^+ or S^+ ions and neutral particles. Given our best time resolution of 2.5 ns, we are unable to observe such phenomena directly.

Note also that at $\lambda = 193$ nm, absorption of the first photon enables the photopredissociation process [10,12,13]:

$$SO_2{}^* \rightarrow SO + O \quad (2)$$

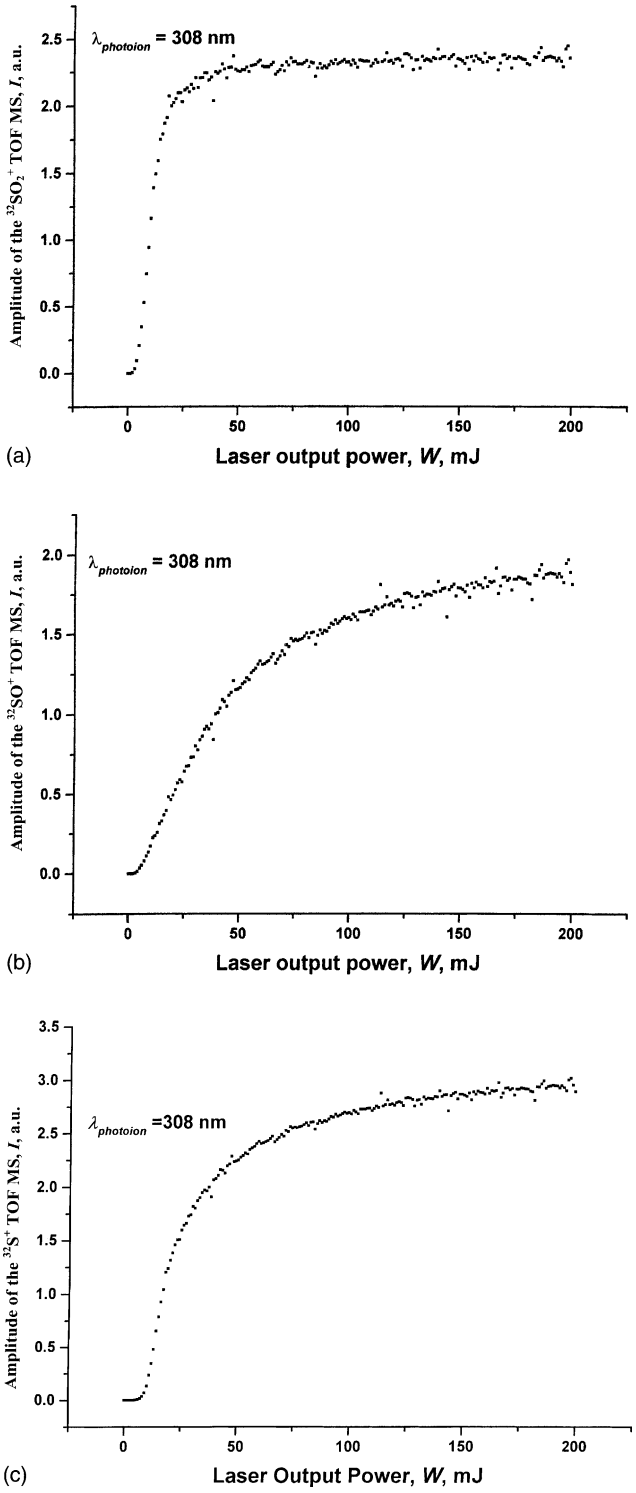

Fig. 5. Dependences of the peak intensity on the laser power measured for the Ar + 20%SO_2 mixture at $\lambda = 308$ nm, $P_0 = 1$ atm: (a) 2—the 64 amu peak (SO_2^+); (b) 2—the 48 amu peak (SO^+); (c) 2—the 32 amu peak (S^+).

while absorption of two photons at $\lambda = 308$ nm induces direct dissociation of SO_2. Thus, the structure of the SO^+ and S^+ peaks of Figs. 2b and 3b should provide important information. Also after photoionization of SO_2 using $\lambda = 193$ nm, the SO_2^+ and SO^+ consist excess of energy, which can be enough for predissociation or dissociation of these ions ($SO_2^+ \rightarrow SO^+ + O$; $SO^+ \rightarrow S^+ + O$). As follows from Fig. 3b and c, the SO^+ and S^+ peaks can be fitted by a single Gaussian at 308 nm, while at 193 nm the SO^+ and S^+ peaks require at least two Gaussian components each, with the respective shift of 25 and 18 ns between components. To provide a qualitative explanation, let us recall that the SO_2 predissociation process at 193 nm proceeds on the nanosecond time scale, while the direct photodissociation after absorption of the second photon at 193 nm develops on the picosecond time scale. This issue cannot be analyzed quantitatively at the moment due to insufficient time resolution.

4.2. Peak amplitude as function of the laser power

4.2.1. Photoionization at 308 nm

In this case, all dependences studied are monotonous curves, which can be fitted by the following expressions, for SO_2^+, SO^+ and S^+, respectively:

$$A_{SO_2^+}(W) = \frac{W^3(a_0 + b_0 W + c_0 W^2)}{1 + W^3(a_0' + b_0' W + c_0' W^2)} \quad (3)$$

$$A_{SO^+}(W) = \frac{W^4(a_1 + b_1 W + c_1 W^2)}{1 + W^4(a_1' + b_1' W + c_1' W^2)} \quad (4)$$

$$A_{S^+}(W) = \frac{W^5(a_2 + b_2 W + c_2 W^2)}{1 + W^4(a_2' + b_2' W + c_2' W^2)} \quad (5)$$

Here, a_i, b_i, c_i, a_i', b_i' and c_i' ($i = 0, 1, 2$) are experimental constants. As follows from the above expressions, SO_2^+ is produced by a third-order process of the laser power at low W, SO^+ is produced by a fourth-order process, and S^+ is produced by a fifth-order process. The saturation effects for these ion-yielding reactions may be interpreted taking into account possible saturation of the $\tilde{A}^1A_2 \leftarrow \tilde{X}^1A_1$ and $\tilde{B}^1B_1 \leftarrow \tilde{X}^1A_1$ optical transitions in SO_2 induced by the 308 nm radiation, along with the photodecomposition of the SO_2^+ and SO^+ ions.

4.2.2. Photoionization at 193 nm

The low laser power section of experimental curves may be fitted by the following expressions, for SO_2^+, the two peaks of the SO^+ ion, and the two peaks of the S^+ ion, respectively:

$$A_{SO_2^+}(W) = a_3 W^2 \quad (6)$$

$$A_{SO^+}^{(1)}(W) = a_4 W^3 \quad (7)$$

$$A_{SO^+}^{(2)}(W) = a_4' W^3 \quad (8)$$

$$A_{S^+}^{(1)}(W) = a_5 W^3 \quad (9)$$

$$A^{(2)}_{S^+}(W) = a'_5 W^3 \quad (10)$$

At higher laser radiation power, maximums appear in every curve. Similar effects have been observed in power dependence of the SO_2 LIF spectrum induced by UV radiation in the 234–237 nm region [23], explained by saturation of the $\tilde{C}^1B_2 \leftarrow \tilde{X}^1A_1$ optical transition in SO_2, and by biphotonic photoionization of the molecule.

5. Conclusions

In the present study, the photoionization spectrum of SO_2 in a molecular beam was studied in detail using radiation of ArF ($\lambda = 193$ nm) and XeCl ($\lambda = 308$ nm) excimer lasers. No signals corresponding to the VdW complexes and clusters of the SO_2 could be detected. The profile of the SO^+ and S^+ peaks could be fitted by a superposition of two Gaussian components for 193 nm photoionization, whereas a single component is for 308 nm excitation. Laser power dependences confirm the multiphotonic nature of photoionization at both wavelengths.

References

[1] D.H. Levy, Adv. Chem. Phys. 47 (1981) 323.
[2] J.F. Garvey, R.B. Bernstein, J. Am. Chem. Soc. 108 (1986) 6096.
[3] J.F. Garvey, R.B. Bernstein, Chem. Phys. Lett. 126 (1986) 394.
[4] R.B. Bernstein (Ed.), Chemical Reactions in Clusters, Oxford University Press, New York, 1996.
[5] R.B. Gerber, A.B. McCoy, A. Garcia-Vela, Annu. Rev. Phys. Chem. 45 (1994) 275.
[6] A.W. Castleman Jr., K.H. Bowen Jr., J. Phys. Chem. 100 (1996) 12911.
[7] S.K. Shin, Y. Chen, S. Nickolaisen, S.W. Sharpe, R.A. Beauder, C. Wittig, Adv. Photochem. 16 (1991) 249.
[8] S. Buelow, M. Noble, G. Radhakrishnan, H. Reisler, C. Wittig, J. Phys. Chem. 90 (1986) 1015.
[9] D.J. Nesbitt, Chem. Rev. 88 (1988) 843.
[10] H. Okabe, J. Am. Chem. Soc. 93 (1971) 7095.
[11] M.H. Hui, S.A. Rice, Chem. Phys. Lett. 17 (1972) 474.
[12] T. Ebata, O. Nakazawa, M. Ito, Chem. Phys. Lett. 147 (1988) 31.
[13] H. Kanamori, J.E. Butler, K. Kawaguchi, Ch. Yamada, E. Hirota, J. Chem. Phys. 83 (1985) 611.
[14] H. Abe, H. Hayashi, Chem. Phys. Lett. 187 (1991) 227.
[15] P.R. Stannard, J. Chem. Phys. 68 (1978) 3932.
[16] A. Matsuzaki, S. Nagakura, Helv. Chim. Acta 61 (1978) 675.
[17] M. Ivanko, J. Hager, W. Sharfin, S. Wallace, J. Chem. Phys. 78 (1983) 6531.
[18] A. Freedman, S.-Ch. Yang, R. Berson, J. Chem. Phys. 70 (1970) 5313.
[19] M. Kawasaki, H. Sato, Chem. Phys. Lett. 139 (1987) 585.
[20] C.S. Effenhauser, P. Felder, J.R. Huber, Chem. Phys. 142 (1990) 311.
[21] W.C. Wang, L.C. Lee, J. Appl. Phys. 58 (1985) 3295.
[22] S.A. Kochubei, K.A. Amosov, V.I. Makarov, I.V. Khmelinskii, Pribori i Tehnika Experimenta 6 (1992) 195.
[23] V.I. Makarov, E. Quinones, J. Photochem. Photobiol. 135 (2000) 1.